Improved understanding of Sodium hydroxide concentration role and kinetic model of cryolite reactive extraction in cathode Spent Pot Linings

Blaž Tropenauer[1*], Dušan Klinar[2], Janvit Golob[3]

[1]*TALUM d.d. Kidričevo, Tovarniška cesta 10, 2325 Kidričevo, Slovenia*
[2]*Scientific Research Centre BISTRA Ptuj, Slovenski trg 6, 2250 Ptuj, Slovenia*
[3]*University of Ljubljana, Faculty of Chemistry and Chemical Technology, Večna pot 113, 1000 Ljubljana, Slovenia*
[*]*Corresponding author: e-mail: blaz.tropenauer@student.um.si*

Spent Pot Lining (SPL) cathode pot, waste from the aluminium smelting process needs detoxification from cyanides, washing out water-soluble salts and extraction of the cryolite (Na_3AlF_6) decomposition products to be recycled. Revealed cryolite decomposition mechanism with NaOH opens possibilities to explore its critical role in the reactive extraction process. Common Na^+ ion from NaOH hinders the solubility of the product but also drives mass transfer to the reaction site. Reaction mass balance provides adequate liquid to solid ratio (L/S) and NaOH concentration range. A newly developed kinetic model based on Whitman film theory and NaOH mass flow enables prediction of the reaction time to decompose cryolite to a low enough level. Results show that the internal particle resistance to transport ($1/k_s$) is 19 times larger than the external ($1/k_l$) one and governs the whole process.

Keywords: Spent pot lining; NaOH concentration role; cryolite decomposition; reaction mechanism; kinetic model.

INTRODUCTION

Hundred thirty years passed since Hall–Héroult electrolytic reduction and smelting process becomes a basic industrial process for the reduction of alumina (Al_2O_3). Nevertheless, the process achieved a significant level regarding energy efficiency and waste product recycling like anodes. Only cathode pot remains systemically unrecycled in many of the production locations around the world, although some technologies for processing exist[1, 2].

Waste is known as Spent Pot Lining (SPL) and derives from each electrolytic cell, or more precisely from the material of the cathode electrode or pot[3–6].

Current European trends regarding hazardous waste streams demand a zero-waste concept and follow effort in aluminium production to complete recovery of SPL streams in a sustainable solution. Besides a waste burden, the material also represents an opportunity to harvest either its energy and/or valuable material content[7].

Residue appears as SPL and is, after mechanical deterioration, sorted to the first cut (FC, mostly carbon) and second cut (SC, mostly chamotte) material.

Since disposal is placed on the base of the wastes hierarchy, some new solutions for waste materials treatment need to be provided. The concept of circular and low carbon economy directs toward the use of materials in the local/regional application chains[8].

The study follows a new, concept of the SPL treatment process. All undesirable substances like NaF and cryolite should be extracted out, and toxic components in the form of cyanides disintegrated. Nontoxic and unreachable product almost without sodium and fluorine can be used in a local circular economy. The new concept introduces no new species in the reaction system, low-temperature processing, low concentrations and no waste streams.

Improved understanding of the NaOH role in a reaction mechanism of the cryolite decomposition and the role of ligands gave, for the first time, the possibility to find the influence of the concentration on a whole process and most significant resistance in the mass transport and chemical reaction chain. Solubility constraint of fluorine ions and common ion effect is theoretically and experimentally determined. Experimental results confirm that the reactive extraction process governs the solubility of its products and internal diffusion resistance inside material particles.

MATERIALS AND METHODS

Both, FC and SC components are declared as hazardous toxic materials (HTM) due to: (i) water leachable fluoride and cyanide salts, (ii) corrosiveness – exhibiting high pH (12) due to content of metallic oxides (Na_2O) and (iii) reaction of carbides, nitrides and Al metal with water and alkaline to form toxic and explosive gases like methane, ammonia and hydrogen (approx. 0.2 l/kg of SPL). Typical chemical composition of average SPL, FC and SC, are summarised in Table 1.

Table 1. Approximate mass composition of whole SPL and mechanical separated first cut (FC); compositions usually variate more than ±10%

Parameter	Amorphous carbon	Graphitized carbon	NaF	Na$_2$O	Cryolite Na$_3$AlF$_6$	CaF$_2$	SiO$_2$	Cordierite	Al$_2$O$_3$	Mullite Al$_6$Si$_2$O$_{13}$	Diaoyudaoite NaAl$_{11}$O$_{17}$	Other
SPL whole mixture composition (unseparated first and second cut):												
Units %	24.7	19.6	9.6	1.3	12.9	2.0	2.6	3.8	2.6	19.0	1.2	0.7
	Carbon part C$_{fix}$ = 44.3%		Water soluble		Mineral part 55.7%							
Mechanically separated first cut of SPL:												
Units %	20.0	33.7	21.5	2.0	12.3	5.0	1.3	–	0.6	–	3.6	–
	Carbon part C$_{fix}$ = 53.7%		Mineral part 46.3%									

Data from Talum d. d. (JSC) company Slovenia

It is necessary to separate both parts at the beginning during mechanical demolition.

Preliminary investigations

Separation of the salts impregnated in carbon and chamotte structure becomes a primary concern while containing most sodium and fluorine salts. Removal of the about 20% of NaF, as a very well solvable strong electrolyte, looks to be the right task for water extraction in the first stage. As SPL contains 1–2% of Na_2F immediate reaction with water gives sodium hydroxide, which raises the pH to more than 12. After NaF removal, cryolite remains as the next massive component in the SPL material with an average value of 13% of the whole sample. With a very low solubility product constant – K_{sp} cryolite, as an almost insoluble component, must be chemically decomposed first to get water-soluble products. Some attempts propose disintegration at higher temperatures[9–11]. The basic concept of industrial application directs experiments toward the low-temperature reactive extraction process with the implementation of no new ionic species into the system. Within the proposed concept, a decomposition of cryolite becomes a central concern in the study. According to the literature, different caustic and acid reactants can also be used for this purpose. To obtain H_2SiF_6 and AlF_3 as the desired component in the electrolytic process Schönfelder[12] chose H_2SO_4 as a solvent. Zhao[13] suggested the same solvent for HF production. Shi Z.[14] used on the other hand 2.5 M NaOH solution with L/S ratio (Liquid to Solid ratio expressed in ml/g and declared as L/S) of 6 to separate cryolite from SPL while Kasireddy[15] used 0.5 to 1.25 M NaOH solution with the preferred L/S ratio of 6.

As the introduction of new ions into the system is not favorable, especially sulphur-based products in the extract, a caustic disintegration of the cryolite takes central attention in the research.

Sodium Hydroxide reacts with cryolite according to a well-known reaction presented with Equation (1) however, reaction steps and mechanism, essential for the design of the process, remain unpublished. This way, preliminary investigations start with batch laboratory tests of FC samples water leaching and searching for a mechanism of cryolite decomposition with sodium hydroxide.

$$Na_3[AlF_6](s) + 4NaOH(aq) \rightarrow 6NaF(aq.)$$
$$+ Na[Al(OH)_4](aq) \tag{1}$$
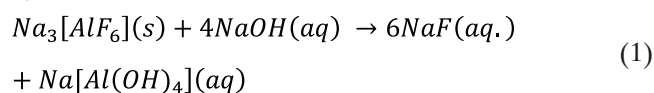
Sodium hydroxide concentration, reaction time and L/S ratio are the main parameters under consideration as they influence most on the results of decomposition and extraction[16] of the cryolite in Equation (2). The use of pure cryolite (97.5 %) eliminates some possible influence of other components on the decomposition mechanism and simplifies mass transfer picture at the surface of the particle. Revealed reaction and mass transport mechanism in this preliminary investigation stage serves as the main model in the central experimental part on origin material as FC samples present.

Reaction mechanism of cryolite decomposition

Cryolite, with its very low solubility of 0.04 % at 20^oC[17], consists of a complex structure in its crystal. Complex anion is formed with fluorine as a ligand arranged in the octahedral structure around a central ion. Ligands contribute electrons to an empty d orbital of the central atom to form a complex anion. As a counterbalance to the negative charge, the compound of the cryolite contains three cations. Decomposition reactions and dissolution, take place during the reactive extraction process, start with cryolite dissociation in water.

To increase the decomposition rate of the cryolite according to Le'Chatelier principle, some products need to be eliminated from the reaction plan. In the first step, toward shifting the reaction to the right, complex anion $[AlF_6]^{3-}$ reacts and disintegrates in hydroxide anion rich solution at high pH (8–12) to $Al(OH)_4^-$ anion or $AlF_x(OH)_{3-x}^-$ anions[16] depending on pH and Al/F ratio in the solution. At low F^- concentrations and high pH values[18] $Al(OH)_4^-$ anion exists, a second step in the reaction of cryolite decomposition can be written as follows by Equation (2).

$$[AlF_6]^{3-} + 4[OH]^- \rightarrow [Al(OH)_4]^- + 6F^- \tag{2}$$

The formation of $[Al(OH)_4]^-$ is confirmed by the stability constant of the Al – OH complexes for this ion (log K = 33). Concerning Al^{3+} – F^- – OH^- the system presented by Sjoeberg[18] indicates the existence of considered species start to appear in the pH range from 8 to 9 and above. The pH of 10 in the samples assures its presence.

As OH^- is a stronger base than F^-, metal ions like Al^{3+} act as strong acids and bind preferentially to hydroxide, therefore, increase the stability of the complex. Also, as can be seen from the spectrochemical series, ($I^- < Br^- < Cl^- < F^- < OH^-$) the crystal field splitting energy (Δ_0) of OH^- is larger than of a F^- ion. Greater Δ_0 contributes to shorter metal-ligand distance as ligands are more strongly attracted to the metal ion and therefore, increased stability of the complex[19].

Finally, as a summary, both reaction steps can be understood as one continuous reaction presented in Equation (1).

Large amounts of sodium and fluorine ions appear as a product, and a lot of sodium hydroxide existing as a reactant seems to be the fundamental characteristic of the whole reaction. Reactions in the presented mechanism are of the ionic type and very fast or almost instantaneous. Consequently, other factors than pure reaction kinetics influence the decomposition reaction rate; in the following part, its analysis becomes the main focus.

Factors affecting the decomposition reaction rate

Firstly, a large amount of appearing sodium ion suggests that the thermodynamic factors like solubility of fluoride ions in sodium hydroxide solution, as the central reactant, play an important role. Phase equilibria governed by Gibbs phase rule and law of mass action help to understand solubility limitation in the complex solution. Phase rule F + P = C + 2 gives P = 2 while only two Phases (P = number of phases) can exist at equilibrium. Three Components (C: H_2O, NaF and NaOH) give three degrees of Freedom (F) of the system, with constant Pressure and Temperature. The selected concentration of NaOH fixes the solubility of the second component

NaF. Variation of common ion enables calculation of the NaF solubility dependence on NaOH concentration.

Secondly, a fulfilled mass balance assures enough sodium hydroxide to disintegrate complete cryolite in the solids. The minimum ratio of L/S (for each concentration) provides enough sodium hydroxide for this purpose. Oppositely, limiting solubility of NaF determines the maximum L/S ratio to assure solubility not to be exceeded.

Thirdly, mass transfer factors contribute mainly to cryolite decomposition reaction resistance of a consecutive reaction path. With combining the first Fick's law and the Whitman film theory, the decomposition kinetics can be modelled and tested in the experimental configuration.

Solution thermodynamics

The common sodium ion does not hinder the cryolite decomposition rate directly but affects solubility due to an instantaneous ionic reaction in the Equation (2). In the heterogeneous system, diffusion of the products and reactants limits the reaction rate. In a consecutive system, the slowest process determines the rate of the whole process. The low solubility of NaF, as a reaction product, limits the diffusion process mostly[16] and limits the entire process. Effect of the common ion in the system under consideration was proposed but not quantified mathematically yet. Such an approach is improved by the implementation of the law of mass action to quantify the solubility equilibrium.

The common Na^+ ion from cryolite (3 ions) and mostly NaOH (4 ions) obstruct the NaF solubility. In water, the NaF solubility at 20°C is 40.6 g/L (0.967 M)[20]. The NaF solubility drops from 0.967 M in water to 0.6 M in 1 M NaOH solution. The solubility product – K_{sp} enables the approximation of the NaF solubility and its dependence on NaOH concentration. This approximation does not consider the ionic strength of the solution and related ionic activity coefficients. NaF solubility – S at various NaOH concentrations – n gives:

$$K_{sp} = [Na^+] \cdot [F^-] = [S + n] \cdot [S] = S^2 + n \cdot S \qquad (3)$$

After the arrangement, the solution of the equation gives the dependence of NaF solubility on NaOH concentration presented in Fig. 5. Calculated results, compared with the experimental results of different authors[20–22], give a reasonably good fit within the uncertainty range of the measured data. Calculated and the Selvaraj results[21] have the largest negative slope of solubility within a range from 0 to 1 M NaOH concentrations and consequently determine the concentration window for the reactive extraction process.

Mass balance and L/S ratio

The Equation (1) gives mass balance for the decomposition and dissolution of the cryolite. L/S ratio was taken as a measure of mass balance to simplify batch experiments design, used rather widely[14]. The minimum L/S ratio provides only the framework of the NaOH mass balance but does not avoid or take into account solubility limit calculated with Equation (3). L/S calculations are always based on (pure) cryolite content in the material processed. Applying (selected) 1 M solution NaOH gives $(L/S)_{min}$ of 19 ml/g. Calculated NaF concentration at 1.5 M NaOH exceeds its solubility limit of 0.57 M as

saturation concentration. To operate below the saturation curve calculated by Equation (3), a larger L/S ratio than a minimal needs to be applied. Calculations in the broader range of NaOH concentrations (0.2 to 1.5 M) directed to the optimal L/S ratio from 50 to 100 ml/g. Concentrations of NaOH in a range of smaller than 1 M and proposed optimal L/S ratios give the frame for experimental arrangements and also for the evaluation of the reactive extraction process.

Process constraints

Before the presentation of work on process kinetics, some significant constraints of the process should to be pointed out:

– The solubility of the cryolite decomposition product – NaF should be kept reasonably below its saturation curve calculated with Equation (3).

– The average reactant NaOH concentration difference from the process start to its end should be high as possible.

– Consequently, a high L/S or substantially larger L/S ratio than minimal should be applied to assure the second constraint – NaOH average concentration high.

The limited solubility of the NaF, as the largest mass part of decomposition reaction in the reactant solution, can hinder by common ion effect the course of the reaction itself. A second product $[Al(OH)_4]Na$ is not limited by its solubility. With the choice of optimal reactant concentration and adequate large enough L/S ratio, all constraints can be avoided.

Mass transfer and decomposition kinetics

Kinetics of the cryolite decomposition inside the amorphous and partly graphitized carbon – coke can be complicated as different types of resistances are possible. A process kinetics modeled on pure cryolite particles can give an elementary reaction field picture, without the influence of other factors. As ionic reactions are very fast, only transport of reactant – NaOH to reaction site and products as NaF to the solution and its solubility determines the process kinetics. The kinetics of the process depends on the reactant concentration, driving mass transfer process around cryolite particles. Combining first Fick's law governing diffusion around particles with Whitman's film theory a modified equation for the mass transfer through the stagnant film – J in $(kg/m^2 \cdot s)$ can be derived by Equation (4). A mass transfer coefficient for liquid in k_l (m/s) is derived from an approximation of differential with concentration gradient – ΔC divided by a stagnant film around particles and its thickness δ_f (m) – a left side of the Equation (4). In the same equation, a NaOH mass flow to particles was equalized with cryolite decomposition rate – a left side of the Equation (5). In further transformation, surface (A) replaces all cryolite particles surface calculated as spherical particles with density (ρ_p) and radius (r_p). Following integration between the mass of cryolite particles $(m_0$ to m) and its decomposition time (0 to t), the equation for cryolite particles decomposition becomes Equation (6).

$$J = -D\frac{dC}{dX} \quad => \quad \frac{dC}{dX} \approx \frac{\Delta C}{\delta_f} \quad => \quad k_l = \frac{D}{\delta_f} \quad => \quad J = k_l \cdot \Delta C \quad (4)$$

$$-\frac{dm}{dt} = k_l \cdot A \cdot \Delta C \quad => \quad A = n_p \cdot A_p = \frac{3m}{\rho_p r_p}$$

$$=> \quad \frac{1}{m} \cdot dm = -\frac{3k_l \Delta C}{\rho_p r_p} \cdot dt \tag{5}$$

$$ln\frac{m}{m_0} = -K \cdot t \quad where \; K = \frac{3k_l \Delta C}{\rho_p r_p} \tag{6}$$

Equation (6) represents a primary tool in the analyses of the decomposition experiments with the cryolite in the pure form and as well as coke particles – FC material (with cryolite inside the matrix) to assess overall mass transfer coefficient. The equation also supports calculation of cryolite decomposition mass balance.

Experiments

To obtain the dependence of decomposition reaction time NaOH on concentration and L/S ratio experiments were performed with pure cryolite and FC with different particles sizes and mixing conditions.

Experiments were performed in two series. The first pure cryolite preliminary series use to confirm its decomposition reaction mechanism in the pure system. In the second series, tests were performed on the real samples of the FC material from the industrial plant. Experiments with FC samples upgrade results to engineering process parameters needed to determine the reactive extraction process.

All experiments were conducted in a batch mixing reactor at 20°C to confirm the possibilities of the extraction process without additional heat consumption. Mass balance calculated as L/S ratio was applied with the access of reactant – NaOH, described above. Selected mixing times from few minutes to several hours cover the whole range of cryolite decomposition. The reactive leaching procedure was performed in a 400 ml low beaker (d_{in} = 78 mm) with 50 mm long magnetic stirrer at a speed of 500 rpm and samples mass in a range of 20 g. Remaining samples were vacuum filtered on a blue ribbon filter paper, dried for 24 h at 120°C and weighed.

The size of FC sample particles largely depends on the application in metallurgical smelting processes, which favour larger particles in a range from 1 to 3 mm than others. For laboratory experiments, smaller particles up to 100 μm are applied. The grinding process needs special attention due to the sticky nature of FC material, which could cause problems[23].

To avoid the common ion effect and consequently, NaF limited solubility samples were first extracted with pure water and wet residues later subjected to reactive alkaline treatment to decompose cryolite and raise the carbon content in the samples to a high level.

Pure Cryolite decomposition tests

Cryolite (Na_3AlF_6) salt of 97.5% purity was grinded to granulation in a range from 10 to 60 μm with d_{50} = 50 μm. The series of experiments were performed at L/S ratio from 50 ml/g with 1 M NaOH to 105 ml/g with 0.2 M NaOH and stirring times of 20, 30, 60, 180 and 300 min.

First cut – FC experiments

Samples were taken from Talum company Al smelter in Slovenia from the electrolysis cell after 6.5 years of operation. Large samples in the form of 20–40 cm wide chunks were taken from the dismantled spent cathode pot. The FC samples were ground in the Retsch MM 400 device to prepare a finer sample with d_{50} = 30 μm. The samples contain merely carbon and compounds like NaF, cryolite, SiO_2, sodium aluminate, CaF_2 and others according to the average composition presented in Table 1.

All the samples were initially extracted with pure water to separate about 23% of the soluble fraction – mainly NaF as salt. Samples were mixed in a batch reactor arrangement as described above, initially for a period of 1h and repeated to extract more than 95% of soluble substances. About 12% of water-insoluble cryolite remained inside the carbon matrix consists of approx. 60% of graphitized and 40% of amorphous carbon. Samples were filtered and dried as described above, before exposure to NaOH reactive extraction.

Fixed-carbon content (C_{fix}) was analyzed in a Mettler Toledo TGA/DSC 1 analyzer by STARe software. After reactive extraction samples were two times washed with water to avoid contamination, filtered and dried before sent to analysis. *X-ray fluorescence (XRF)* was used for elementary quantitative analysis and measured on Thermo ARL Advant'X XRF with copper tube operated at 50 kV and 60 mA. *X-ray diffraction (XRD)* was used for solid crystal phase identification using a Panalytical Cubix3 X-Ray Diffractometer equipped with an X'Celerator detector. The copper tube operated at 50 kV and 40 mA. Qualitative and quantitative analysis with the *Rietveld method* was used to obtain the mass fractions of the compounds analyzed by X'Pert PRO x-ray powder diffractometer with Cu – Kα1 radiation in the 2Theta range from 5 to 90° and with a step of 0.017°, 0.7 s/step – time per step and 59 min scan time.

The alkali leaching experiments were conducted with two limited concentrations of NaOH 0.3 and 1 M and corresponding L/S ratio of 21 and 15 ml/g at stirring times of 9, 30, 60 and 180 min.

RESULTS AND DISCUSSION

Experiments with pure cryolite

First series of the experiments conducted at different concentrations of NaOH solution, at L/S 50 ml/g and reaction times up to 5 hours where more than 92% of the cryolite was decomposed and dissolved. The results of the remaining cryolite mass indicate the process transition point at 3 hours, where decomposition slows down to a substantially low rate.

Diminishing of the remaining cryolite after 3 hours of reaction with NaOH in the whole testing range is technically negligible slow and cannot be solved in the same contacting system. Solutions can be twofold, change mixing contacting system to counter current or leaves a small amount of the cryolite undecomposed.

The significance of the NaF solubility potential, measured as the percentage of actual concentration below the saturation point is presented in Fig. 1. Results suggest

a)

b)
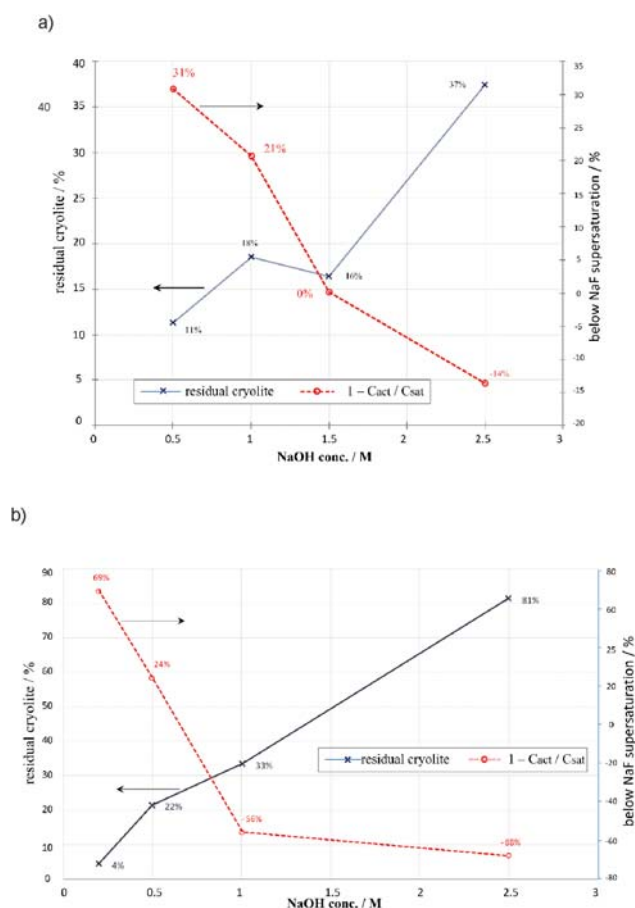
Figure 1. Residual Cryolite in % in different *NaOH* solution
and: a.) L/S = 50 ml/g – mean 3.15 times (L/S)$_{min}$ on
average and 60 min, b.) L/S taken 1.13 times (L/S)
$_{min}$ and reaction time 180 min

inverse proportional relation of a difference between the
actual and saturated concentration of NaF at applied
reactant concentration. The same relation can be seen at
three time's larger reaction times 1:3 and L/S ratio 3:1.
At these conditions, the level of cryolite decomposition
is higher even at three time's shorter reaction time what
confirms the importance of L/S ratio. High level of L/S
ratio above (L/S)$_{min}$ assures high average concentration
potential of the NaOH even at the end of the reaction
and provides enough space for reaction products like NaF.

According to results, a series of close to optimal experi-
ments were performed in a lower range of concentration
– 0.3 M NaOH and L/S of 90 ml/g 1.43 times (L/S)$_{min}$.

Analysis of the process kinetics, according to Equation
(6) presented in Fig. 2 gives proportional factor K as
$5.94 \cdot 10^{-4} \cdot s^{-1}$. With given data for cryolite particles as
$\rho_p = 3 \cdot 10^3$ kg/m³, $r_p = 2.5 \cdot 10^{-5}$ m and $\Delta C_{av} = 9.2$
kg/m³ (in a range from 0.3 M to 0.105 M at the end)
a mass transfer coefficient k_l was calculated as $1.61 \cdot 10^{-6}$
m/s. The calculated value of k_l is in confirmation with
published values for ionic species in water. The result
enables discrimination among resistance in the liquid film
around the particle and resistance in the pores inside
particles at experiments with the first cut – FC material.

Decomposition of the cryolite in a first cut sample

First cut material (FC) with the average composition
presented in Table 1 and d50 = 30 μm granulation was
initially extracted with water to eliminate originally pre-
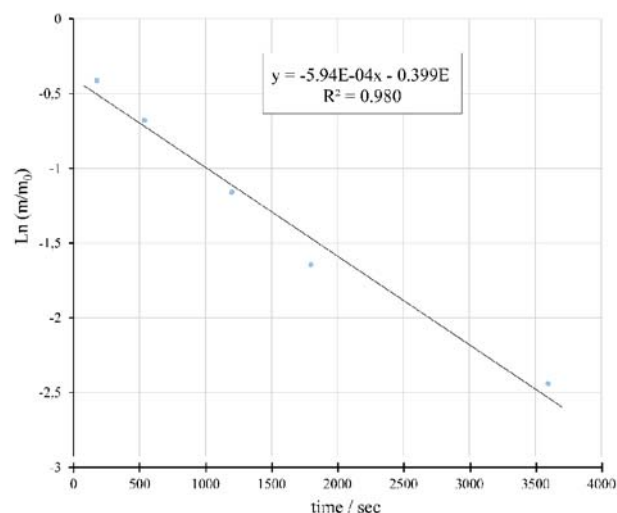
Figure 2. Decomposition kinetics of pure cryolite sample
calculated by Equation (6) in 0.3 M *NaOH* solution
and L/S of 90 ml/g 1.43 times (L/S)$_{min}$

sented NaF. Elimination of the originated NaF avoids
hindering the alkali reaction of cryolite decomposition
and extraction from the FC carbon matrix.

Initially, water leached FC samples were reacted with
1M NaOH solution at L/S of 15 ml/g (3.4 times (L/S)$_{min}$
– calculated on cryolite content) and 3 h mixing time.
An XRD diffractogram analysis presented in Fig. 3
indicates the disappearance of cryolite[24]. Quantitative
analysis acc. to Rietveld gives 5.1% of cryolite at the
end from 23.1% at the beginning, which means 78%
removal of the cryolite.
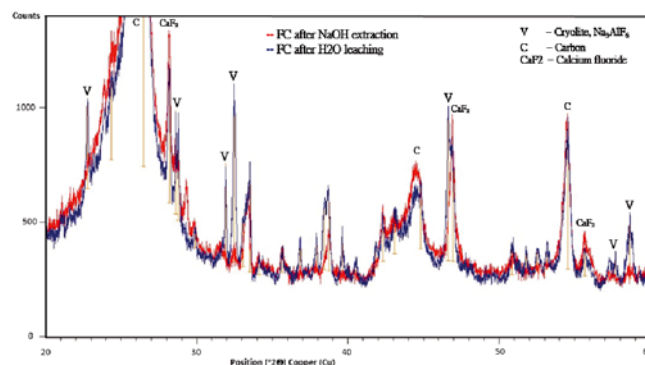
Figure 3. Diffractograms of an effective cryolite decomposition:
pixels (V): 32 and 32.5; 57.8 and 58.7 have a lower
value on the red line after alkali leaching step. Cry-
stallographic data from ICCD: carbon 00-008-415,
CaF$_2$ 03-065-0535, cryolite 00-025-0772

Sample of FC contains initially 72.2% of carbon and
rises to 79.6% after NaOH reaction, insoluble compo-
nents like CaF$_2$ – 7.4% and diaoyudaoite – NaAl$_{11}$O$_{17}$
– 3.9% remains.

Next FC leaching experiment at the same conditions
as with pure cryolite on Fig. 2 with 0.3 M NaOH and
L/S of 21 ml/g (based on cryolite content) 1.43 times
(L/S)$_{min}$ indicates a steady reduction of cryolite in the
FC sample with time. XRD quantitative analysis from
3 h comparable mixing time gives 7.4% of cryolite at
the end from 23.1% at the beginning; 68% of cryolite
was removed. Initial carbon content rises from 72.2% to
83%, a larger rise of C$_{fix}$ in the second experiment can

be related to larger L/S ratio of 21 ml/g comparing to 15 ml/g. More water probably dissolves some remained water leachable components from particles.

Process kinetics analysis with Equation (6) from Fig. 4 gives proportional factor K as $6.35 \cdot 10^{-5} \cdot s^{-1}$. A decade smaller number suggests larger overall resistance of the species transport into the graphitized coke particles and products backward to the solution. With the data for graphitized coke: $\rho = 2.2 \cdot 10^3$ kg/m³, $r_p = 1.5 \cdot 10^{-5}$ m and $\Delta C_{av} = 8.4 \cdot$ kg/m³ (from 0.3 M to 0.15 M at the end) overall mass transfer coefficient – K_o becomes $8.32 \cdot 10^{-8}$ m/s. Mass transfer coefficient for FC consists of two parts: (i) transport from bulk liquid to particle surface (the same case as in pure cryolite) and (ii) transport inside solid carbon matrix. Adequately, K_o consists of two resistances: resistance of the transport to the surface (in the liquid film around particles) and inside solid particles (resistance in solid). Assuming the replacement of the external resistance by previously calculated value for pure cryolite the internal resistance, inside the particle can be calculated. Results of internal resistance $1/k_s = 1.2 \cdot 10^7 \cdot$ s/m, and external $1/k_l = 6.2 \cdot 10^5 \cdot$ s/m indicates that resistance to diffusion inside solid particles is 19 times higher than in liquid. Such basic information opens possibilities to the development of the SPL treatment process, to find an adequate contacting method and other corresponding technological parameters supported by chemical engineering knowledge.

Solubility diagram Fig. 5 based on Equation (3) and data from Selvaraj[21] gives the possibility to represent mass balance in the liquid phase. The process starts on the abscissa and ends on the ordinate axis. Different NaOH concentrations give larger $(L/S)_{min}$ ratios which at 0.6 exceed the solubility curve at the end of a process and should operate at a larger L/S ratio than minimal.

Comparable results of the cryolite disintegration are possible to be achieved with FC samples where remaining cryolite content is left in the range between 5% and 10% (of whole FC sample) at the process conditions discussed above. These material quality specification frames open two general issues with imposed answers:

1. What is the optimal particle size of the SPL material needed? Answer: main selection criteria should follow application possibilities and corresponding particle size specifications.
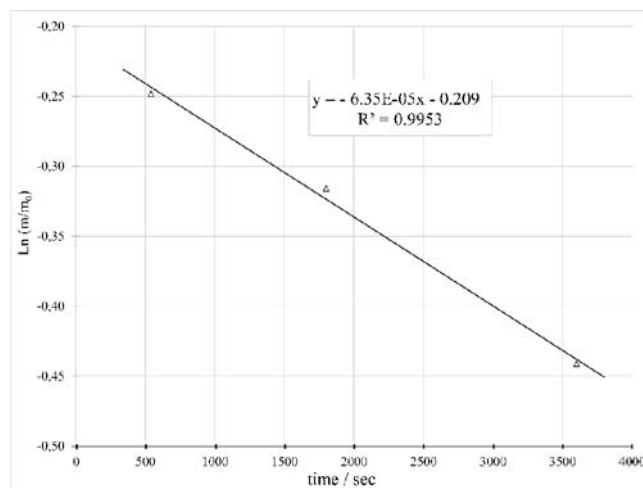
Figure 4. Decomposition kinetics of FC sample calculated by Equation (6) in 0.3 M *NaOH* solution and L/S 21 ml/g (based on cryolite content) 1.43 times $(L/S)_{min}$
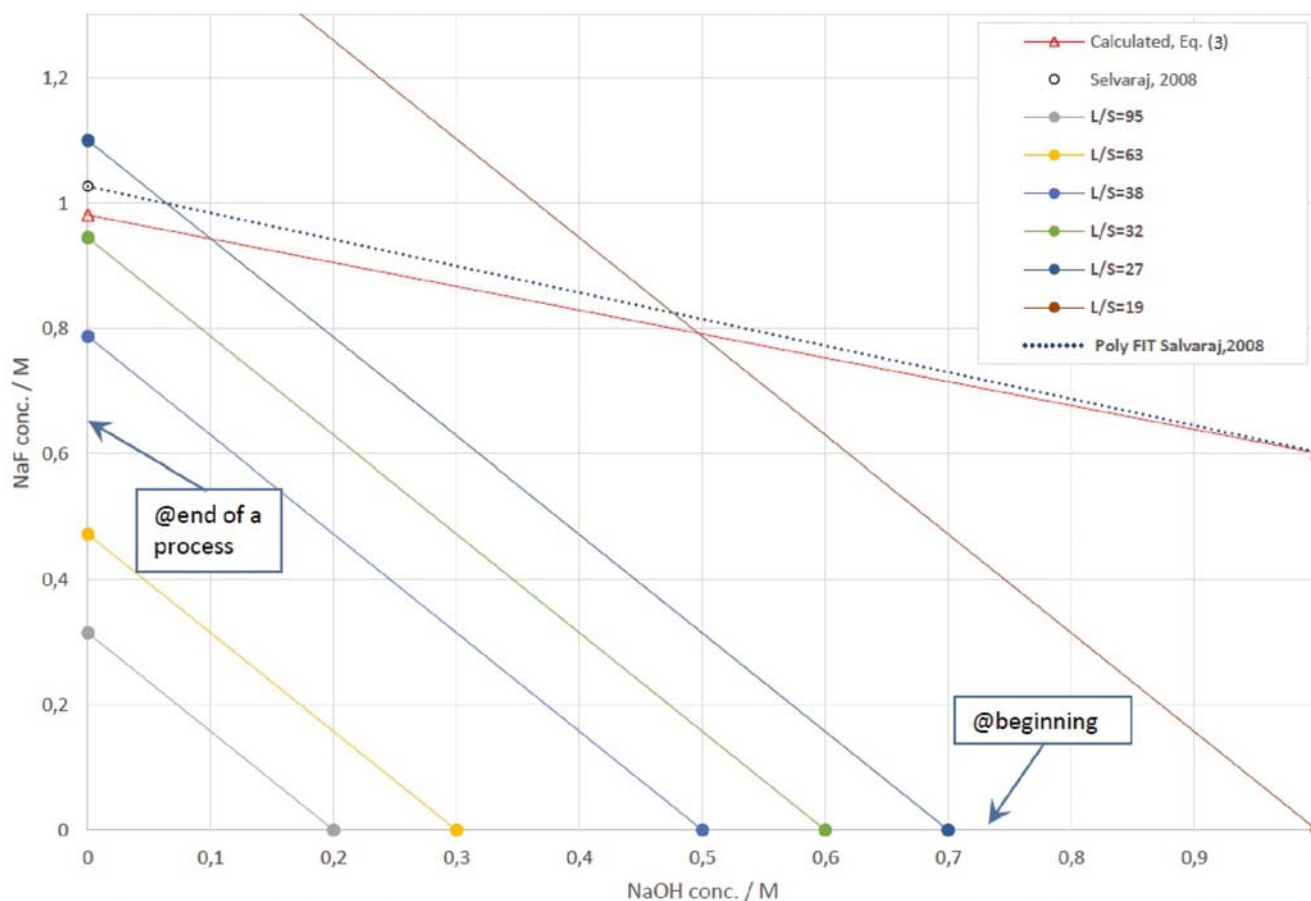
Figure 5. Diagram of *NaF* conc. in *NaOH* solution presented as liquid phase mass balance diagram with different $(L/S)_{min}$ ratios at the start and end of a process

2. Results and evidence support the suggestion that process and economical optimum of final product quality lies in the range of $10\% > C_{cyolite} > 5\%$ and $C_{fix} \geq 80\%$ with no water leachable and toxic components. Response: explore application possibilities of the SPL – FC and SC material with proposed composition to find related particle size requests.

CONCLUSIONS

With the revealing of the alkaline cryolite decomposition reaction mechanism and corresponding process kinetics model, a basis for the development of a reactive extraction process of SPL is established. Complex, but valuable waste materials like SPL, need to be prepared – processed before entering into a local chain of a circular economy. Complex material also needs a straightforward combination of mechanical and chemical procedures to gain a marketable and environmentally acceptable material as sustainable application.

Reaction mechanism with ligand exchange to complex aluminium ion and the common ion effect on solubility in reactant solution are the key parameters in the first part of the process. The water extraction step eliminates originally presented product – NaF to enable cryolite decomposition reaction and transport of reactant – NaOH and products, mainly NaF, by diffusion running process into bulk extraction liquid solution. Keeping NaOH concentrations low between 0.1 to 0.3 M, without introducing new ionic species into the reaction and extraction system and operation at room temperatures simplifies the process and contributes to its economics. This NaOH concentration range is also within the range proposed in the patent applied to the Slovenian Intellectual Property Office (SIPO)[25].

The experiments with pure cryolite allowed the quantification of the mass transfer coefficients related to the NaOH transfer from the solution to the surface of the cyolite particles. In the case of the SPL material, the cryolite is dispersed inside particles, the mass transfer coefficient of NaOH also includes its diffusion within the SPL particle.

As the kinetic modeling and measurements give the internal resistance, inside the particle, 19 times larger than the external one (in liquid phase), larger resistance governs the time of the overall process of decomposition and extraction. Such process circumstances impose careful selection of the technology, process and equipment adequately, according to the primary recognition learned that diffusion governs the process.

Composition of the final product with high carbon content – $C_{fix} > 80\%$, some amount of CaF_2 and a small part of remaining cryolite with alumina and silicates direct application possibilities toward metallurgy, cement, mineral wool production and others. Particle size mostly depends on the application and needs to be adapted thoughtfully.

ACKNOWLEDGMENTS

NOMENCLATURE

A	surface area of cryolite sample (m^2),
A_p	surface area of cryolite particle (m^2),
C	number of Components,
$C_{cryolite}$	cryolite content (%),
C_{fix}	fixed carbon content (%),
D	diffusivity ($m^2 \cdot s^{-1}$),
d_{50}	average particle diameter (μm),
F	number of degrees of Freedom,
FC	First Cut,
HTM	Hazardous Toxic Materials,
ICCD	ICCD type of camera,
J	mass flux through the stagnant film ($kg \cdot m^{-2} s^{-1}$),
K	proportional factor in Eq. 6 – $K = \frac{3k_l \Delta C}{\rho_p r_p}$ (s^{-1}) (s^{-1}),
K_o	overall mass transfer coefficient – $K_o = \frac{1}{\frac{1}{k_l}+\frac{1}{k_s}}$ ($m \cdot s^{-1}$),
k_l	individual liquid phase mass transfer coefficient ($m \cdot s^{-1}$),
k_s	individual solid mass transfer coefficient ($m \cdot s^{-1}$),
K_{sp}	Solubility product constant ($mol^2 \cdot dm^{-6}$),
L/S	Liquid to Solid ratio ($ml \cdot g^{-1}$),
$(L/S)_{min}$	minimum liquid to solid ratio ($ml \cdot g^{-1}$),
m	mass of cryolite sample (g),
m_0	the initial mass of cryolite sample (g),
n_p	number of cryolite particles in cryolite sample
P	number of phases,
r_p	radius of cryolite particle (μm),
SC	Second Cut,
SPL	Spent Pot Lining,
t	time of cryolite decomposition (s),
XRD	X-ray Diffraction, identifies type and amount of mineral phases in the sample,
XRF	X-ray Fluorescence, gives information on elemental composition of sample,
δ_f	thickness of stagnant film around particles (μm),
ρ_p	density of cryolite ($kg \cdot m^{-3}$),
ΔC	concentration gradient ($kg \cdot m^{-3}$),
$1/k_l$	external resistance in the liquid film around particles ($s \cdot m^{-1}$),
$1/k_s$	internal resistance inside solid particles ($s \cdot m^{-1}$).

LITERATURE CITED

1. Holywell, G. & Breault, R. (2013). An overview of useful methods to treat, recover, or recycle spent potlining, JOM. 65, 1441–1451. DOI: 10.1007/s11837-013-0769-y.

2. Pawlek, R.P. (2012). Spent Potlining: An Update, in: Light Met., 2012. DOI: 10.1002/9781118359259.ch227.

3. Chauke, L. & Garbers-Craig, A.M. (2013). Reactivity between carbon cathode materials and electrolyte based on industrial and laboratory data, Carbon N. Y. 58, 40–45. DOI: 10.1016/j.carbon.2013.02.023.

4. Hop, J.G., Støre, A., Foosnæs, T. & Øye, H.A. (2004). Chemical and physical changes of cathode carbon by aluminium electrolysis, VII Int. Conf. Molten Slags Fuxes Salts. 775–782. DOI: 10.1179/037195505X63376.

5. Østrem, Ø. (2013). Cathode wear in Hall-Héroult cells, Thesis for the degree of PhD, Norwegian University of Science and Technology, Faculty of Natural Sciences and Technology, Department of Materials Science and Engineering.

6. Silveira, B.I., Dantas, A.E., Blasquez, J.E. & Santos, R.K.P. (2002). Characterization of inorganic fraction of spent potliners: Evaluation of the cyanides and fluorides content, *J. Hazard. Mater*. 89, 177–183. DOI: 10.1016/S0304-3894(01)00303-X.

7. Mikša, D., Homšak, M. & Samec, N. (2003). Spent potlining utilisation possibilities, *Waste Manag. Res*. 21, 467–473. DOI: 10.1177/0734242X0302100509.

8. Tropenauer, B., Klinar, D., Samec, N. & Golob, J. 2018. Circular economy model of cathode waste processing. DOI: 10.18690/978-961-286-211-4.8.

9. O'Neil, M.J. (ed.), (2001). The Merck Index – An Encyclopedia of Chemicals, Drugs, and Biologicals. 13th Edition, Whitehouse Station, NJ: Merck and Co., Inc., p. 456.

10. Cenčič, M., Kobal, I. & Golob, J. (1998). Thermal Hydrolysis of Cyanides in Spent Pot Lining of Aluminium Electrolysis, *Chem. Eng. Technol*. 21, 523–532. DOI: 10.1002/(SICI)1521-4125(199806)21:6<523::AID-CEAT523>3.0.CO;2-P.

11. Ntuk, U., Tait, S. White, E.T. & Steel, K.M. (2015). The precipitation and solubility of aluminium hydroxyfluoride hydrate between 30 and 70°C. *Hydrometallurgy*, 155, 79—87. DOI: 10.1016/j.hydromet.2015.04.010.

12. Schönfelder, I., Gock, E. Tochtrop, E. & Schmidt Rieder, E. 2015. Recycling von Elektrolyseausbruch (SPL) aus der Primäraluminiumgewinnung, (n.d.). http://www.vivis.de/phocadownload/Download/2015_rur/2015_RuR_385-404_Gock.pdf (accessed June 15, 2018).

13. Zhao, L.C. 2001. Comprehensive recovery of waste linings of aluminium electrolysers, CN patent 1,320,491 (Appl. date 28 February 2001). https://patents.google.com/patent/CN1320491A/en.

14. Shi, Z., Li, W. Hu, X., Ren, B., Gao, B. & Wang, Z. (2012). Recovery of carbon and cryolite from spent pot lining of aluminium reduction cells by chemical leaching, *Trans. Nonferrous Met. Soc. China*, 22, 222–227. DOI:10.1016/S1003-6326(11)61164-3.

15. Kasireddy, V., Bernuer, J.L. & Kimmerle, F.M. (2003). Recycling of spent pot linings, US patent No.: US 6,596,252 B2, Date of Patent: Jul. 22, 2003.

16. Lisbona, D.F. & Steel, K.M. (2008). Recovery of fluoride values from spent pot-lining: Precipitation of an aluminium hydroxyfluoride hydrate product, *Sep. Purif. Technol*. 61(2), 182–192. DOI: 10.1016/j.seppur.2007.10.012.

17. NIOSH – The National Institute for Occupational Safety and Health. 2016, Solubility of Cryolite, (2016). access on 10. Jun 2018 https://www.cdc.gov/niosh/npg/npgd0559.html.

18. Staffan Sjoeberg, Chemical Specification in Aqueous Al^{3+}-F^--OH^- Systems of relevance to Natural Waters and Body Fluids: The dissolution of AlF3 and Na3AlF6 (cryolite). Department of Inorganic Chemistry, Umeå University, Sweden. Unpublished report for Toxicon AB, (2002). (Committee for Risk Assessment RAC Annex 1 Background Document to the Opinion proposing harmonised classification and labelling at Community level of Trisodium hexafluoroaluminate (cryolite), natural and synthetic; 2010).

19. Averill, B. & Eldredge, P. (2016). General Chemistry: Principles, Patterns, and Applications 1.0 |Flat World Education, Flat World Educ.

20. Reynolds, J.G. & Belsher, J.D. (2017). A Review of Sodium Fluoride Solubility in Water. *J. Chem. Eng*. 62(6), 1743–1748. DOI: 10.1021/acs.jced.7b00089.

21. Selvaraj, D., Toghiani, R.K. & Lindner, J.S. (2017). Solubility in the Na + F + NO3 and Na + PO4+ NO3 Systems in Water and in Sodium Hydroxide Solutions. *J. Chem. Eng*. 53(6), 1250–1255.DOI:10.1021/je700597m.

22. Weber, C.F., Beahm, E.C., Lee, D.D. & Watson, J.S. (2000). A Solubility Model for Aqueous Solutions Containing Sodium, Fluoride, and Phosphate Ions, *Ind. Eng. Chem. Res*. 39(2), 518–526. DOI: 10.1021/ie990457l.

23. Xiping, C. & Wangxing, L. (2007). Research on crushing character of spent cathode, in: TMS Light Materials.

24. Tropenauer, B., Klinar, D., Samec, N., Golob, J. & Kortnik, J. (2019). Sustainable waste-treatment procedure for the spent potlining (SPL) from aluminium production. *Mater. Tehnol*. 53(2), 277–284. DOI: 10.17222/mit.2018.147.

25. Patent application No.: P-201900265, Slovenian Intellectual Property Office (SIPO), (January 6. 2020).